Local Packing Disorders in a Polymer Crystal by Two Dimensional Solid-State NMR

Toshikazu Miyoshi,*,† Wei Hu,† and Hideaki Hagihara‡

Research Institute of Nanotechnology and Research Institute for Innovation in Sustainable Chemistry, National Institute for Advanced Industrial Science and Technology (AIST), Central 5-1 Higashi 1-1-1, Tsukuba, Ibaraki 305-8565, Japan

Received March 1, 2007
Revised Manuscript Received August 3, 2007

Isotactic polyolefins are semicrystalline polymers, and the polymer chains in the crystalline regions adopt helical conformations with right (*R*) or left (*L*) handed senses, and it is possible for the chains to independently adopt upward or downward orientations along *c*-axis.[1−5] Upward and downward orientations are defined in terms of differences between the *z* coordinate of the first lateral carbon, which is directly connected to the main-chain CH carbon, and the *z* coordinate of the main-chain CH carbon. This disorder commonly occurs in stereoregular crystalline polymers. The crystal structure of isotactic-poly(3-methyl-1-butene) (iP3M1B) has been investigated by XRD.[5,8−10] All XRD results commonly indicated that iP3M1B adopts uniform 4_1 helical conformations. The most recent XRD investigation by Corradini, P. et al. revised that four uniform 4_1 helices are packed into a $P2_1/b$ monoclinic space group with unit parameters of $a = 9.55$, $b = 17.08$, $c = 6.84$ Å, and $\gamma = 116.3°$;[5] however, they could not conclude that either full limit order or full limit disorder related to the up and down orientations in the iP3M1B crystal existed, due to insufficient fiber diffraction resolution.

High-resolution solid-state (SS) NMR has been successfully utilized for local structure analysis of polymers in the crystalline region as a comprehensive tool of XRD analysis.[6,7,11−18] Structural disorders such as conformations and regio- and stereo-defects in the crystalline region have been quantatively characterized by high-resolution SS NMR.[6,7] The packing structures of the crystalline polymers were also investigated by high-resolution SS NMR[12−18] However, the observed NMR line shapes were attributed simply to symmetry of space group in full limit order, were not related with the packing disorders due to up and down orientations.[18] This might be attributed to very minor structural change due to substitution of up- and downward chains and insufficient NMR spectral resolutions. Therefore, improvement of the spectral resolution would be a key to elucidating real packing structures as well as further SS NMR analysis for understanding the crystal structures. In the past decade, a number of NMR techniques (e.g., fast magic-angle spinning (MAS),[19,20] powerful decoupling,[21] very high magnetic field,[22] and 2D chemical shift correlations[23−25]) have been developed to improve spectral resolution and/or sensitivity. Combined use of modern techniques may allow us to obtain further structural information for the polymer crystals.

In this communication, we apply two-dimensional (2D) refocused $^{13}C-^{13}C$ INADEQUATE technique through *J*-mediated interaction[25] and two-phase pulse modulated (TPPM)[21] decoupling to the iP3M1B crystal at a low temperature of 233 K. Consequently, we succeeded in significant improvement in NMR spectral resolution and will investigate the packing structures included in the iP3M1B crystal through the resolved NMR signals. We conclude that a combination of symmetry of space group and up and down disorders lead to multiple peaks which are sources in the different packing structures, and local packing disorder is interpreted in terms of NMR signal intensities.

Figure 2 shows the ^{13}C high-resolution melt-state[26] and SS NMR spectra for iP3M1B, and the signal assignment is referred to in the literature.[15,26,27] In the case of the melt state, individual carbons show almost single resonances which were attributed to a highly stereoregular iP3M1B with a *mm* > 96%.[26] High-resolution SS NMR spectrum was obtained by incorporating a ^1H spin−lattice relaxation time in the rotating frame ($T_{1\rho H}$) filter of 15 ms, which filters out the amorphous signals, and consequently, selectively observes the crystalline signals. The crystalline signals show different chemical shifts from those in the melt state, reflecting rigid 4_1 helical conformations. In addition, the C4 and C5 signals show a chemical shift separation of ∼ 6 ppm. The C5 carbon shows *gauche*−*gauche* conformations with respect to the two C1 carbons in the γ positions, whereas the C4 carbon has a *trans*−*gauche* conformation with respect to the two C1 carbons.[5] Therefore, the observed upfield shift of the C5 signals is interpreted in terms of one additional γ *gauche* effect.[15,28] In addition, the main-chain signals of C1 and C2 show almost a single resonance with relatively broad linewidths compared with those of the side-chain signals. On the other hand, the side-chain C3, C4, and C5 signals apparently show 3, 5, and 3 distinguishable peaks, each signal spanning a chemical shift range of ≈ 2.4 ppm, due to the packing effects. It should be noted that the observed shift range due to packing effect is the largest among the previously reported results.[12−17] The observed multiple peaks for individual side-chain carbons are coalesced into one at temperatures above 353 K, and all the main- and side-chain signals show maximum line broadenings at further high temperatures (data are not shown). These line-shape changes are attributed to overall chain dynamics in the crystalline region, which is related to mechanical relaxation.[29] In addition, the DSC curve shows only one endothermic peak with a melting peak center of 577 K.[26] These dynamic and thermal results indicate the observed multiplicities in the side-chain ^{13}C signals arise from one crystal form.

We constructed two packing models, namely, full limit order and full limit disorder, on the basis of the previous X-ray result.[5] In full limit order, iP3M1B chains at individual sites show one given chirality with up- or down-ward orientation, namely, a *right*-handed chain with upward orientation (R_u) or a *left*-handed chain with downward orientation (L_d). The atomic coordinates in our study are consistent with the previous XRD analysis. In this full limit order, low symmetry of unit cell provides two types of the packing structures. For example, two types of C5 carbons labeled by C5I and II and colored by red are shown in Figure 1a. The different packing structures lead to different atomic distances (carbon−carbon and carbon−proton) with the adjacent chains. Here, we simply show the carbon−carbon atomic distances depending on the packing structure, since we are currently investigating $^{13}C-^{13}C$ space correlation for ^{13}C labeled iP3M1B. This information directly reflects the packing structures of the iP3M1B chains in the crystalline region. This

* Corresponding author. E-mail: t-miyoshi@aist.go.jp.
† Research Institute of Nanotechnology, National Institute for Advanced Industrial Science and Technology (AIST).
‡ Research Institute for Innovation in Sustainable Chemistry, National Institute for Advanced Industrial Science and Technology (AIST).

10.1021/ma070518o CCC: $37.00
Published on Web 08/18/2007

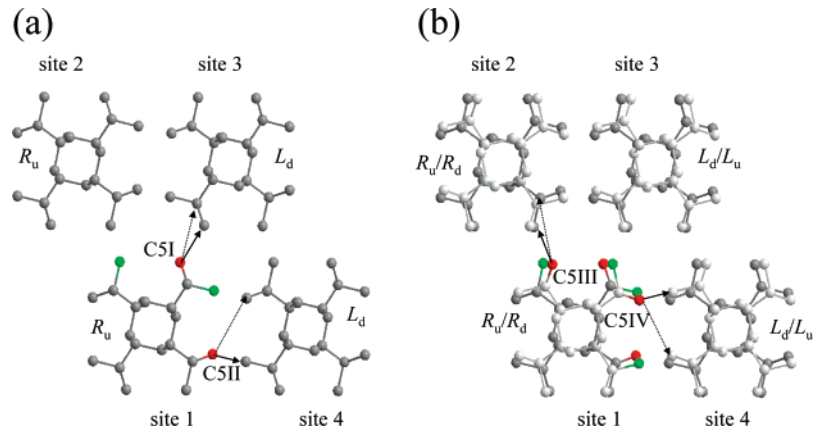

Figure 1. Two packing structures for full limit-order (a) and full limit-disorder (b) models proposed by XRD analysis.[5] The C5 and C4 carbons in site 1 are colored by red and green, respectively. In full limit order, C5I and C5II carbons in site 1 show closest and second closest contact distances of 3.83 and 3.84 Å, respectively, with the carbons of L_d chain in site 3, and 3.52 and 3.62 Å with carbons of L_d in site 4, respectively. In full limit disorder, C5I, C5II, C5III, and C5IV carbons show closest and second closest contact distances of 3.83 and 3.84 Å with respect to the carbons in the adjacent chains (counter chain, L_d, site 3) and 3.72 and 4.40 Å (L_u, site 3); 3.52 and 3.62 Å (L_d, site 4) and 3.56 and 3.70 Å (L_u, site 4); 3.94 and 4.04 Å(R_u, site2) and 4.06 and 4.16 Å (R_d, site 2); and 3.56 and 4.02 Å (L_d, site 4) and 3.52 and 3.84 Å (L_u, site 4), respectively. The full limit-order model shows two environments of packing structures, whereas the full limit-disorder model indicates eight environments. The solid and dotted arrows indicate the closest and second distances, respectively, with respect to the carbons in the adjacent chains. The two models were prepared by Chem Draw ver. 9.1.

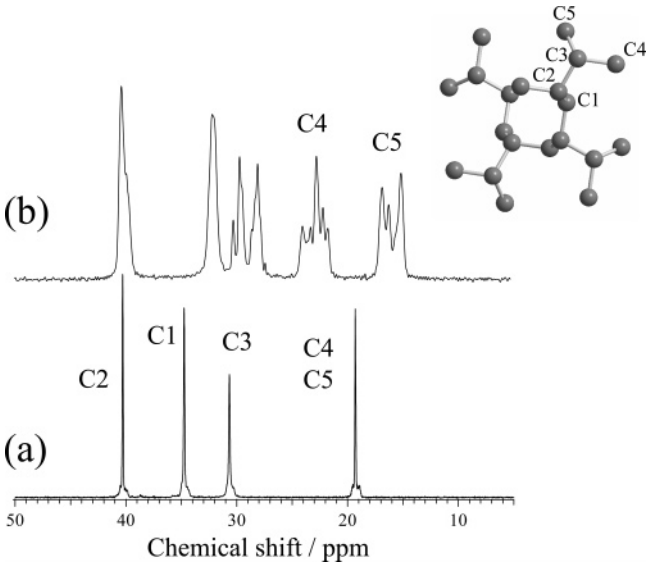

Figure 2. ^{13}C high-resolution (a) melt-state and (b) SS NMR spectra for iP3M1B at 588 and 233 K, respectively. The melt-state and SS NMR spectra were obtained at 75.6 MHz on a BRUKER AVANCE 300 spectrometer using 4 and 7 mm double resonance high-temperature probes, respectively. In the melt state, the experimental conditions are as follows: MAS, 3.5 kHz; 90° pulse, 4.5 μs; recycle delay, 500 ms; acquisition (ACQ) time, 150 ms; continuous wave decoupling, 50 kHz; duty cycle, 23%. In the experiment of high-resolution SS NMR, the iP3M1B sample was crystallized isothermally at 553 K. A spin−lattice relaxation time in the rotating frame ($T_{1\rho H}$) filter with a spin-locking time of 15 ms under a field strength of 65 kHz, which suppresses amorphous signals, was utilized for obtaining a high-resolution SS NMR spectrum of pure crystalline signals. The other experimental conditions were as follows: MAS frequency, 3 kHz; cross-polarization (CP) time, 1 ms; recycle delay, 1.5 s; ACQ time, 61 ms; TPPM-15 decoupling, 70 kHz. A signal assignment is also inserted.

work will be published in a future. The C5I carbon of R_u chain in site 1 shows the closest and second closest contact distances of 3.83 and 3.84 Å, respectively, with the side-chain carbons in adjacent L_d chain in site 3. On the other hand, C5II carbon in site 1 shows the closer packing structure with the distances of 3.52 and 3.62 Å, respectively, with the carbons in the adjacent L_d one in site 4. Presence of two packing structures reflects low symmetry of monoclinic lattice. In full limit disorder, upward and downward orientations statistically occur in individual sites. The procedures for substitutions of up and down chains are the following: First, the original chains are rotated by 180° around an arbitrary axis in the plane including *c*-axis, and which is perpendicular to the *c*-axis and parallel to *b*-axis. Then, the rotated chains were translated along *c*-axis so that each methyl carbon has the same *z* coordinate with one of the original chains. These procedures are the same as in the original work[5] and other systems such as isotactic polypropylene[2] and isotactic poly(1-butene).[1] We did not perform further structural energy minimization on the full limit-disorder structure. In full limit disorder, as shown in Figure 1b, C5I and C5II carbons show the same distance sets as those in the limit-order model. In addition, we obtained two more distance sets with respect to the side-chain carbons of contrary orientation of the counter L_u chain, in site 3 (3.72 and 4.40 Å) and those of the L_u chain, in site 4 (3.56 and 3.70 Å), respectively. In addition, orientation disorder in site 1, say that, replacing the R_u chain by the R_d chain, apparently induces two additional environments for the C5 carbons, namely, C5III and C5IV as shown in Figure 1b. The C5III carbon of the R_d chain in site 1 shows the different distance sets of 3.94 and 4.04 Å, and 4.06 and 4.16 Å with the side-chain carbons of the counter R_u and R_d chains, respectively, in site 2 (Figure 1b). Similarly, the C5IV carbons have two distance sets of 3.56 and 4.02 Å, and 3.52 and 3.84 Å with respect to the side-chain carbons in the L_d and L_u chains, respectively, in site 4. The obtained distance sets are summarized in Table 1. The structural factors both of low symmetry of monoclinic and orientation disorders result in a total of eight packing structures with different distance sets. The same number of contact-distance sets is obtained for the side-chain C4 carbons. Here, note that our contact-distance analysis is limited to two close contact distances from one adjacent chain, and remote distance effects from the other chains are ignored. Under these conditions, full limit order and full limit disorder models provide two and eight packing structures, respectively. The number of peaks, 3, 5, and 3, for the C3, C4, and C5 carbon signals, respectively, in the high-resolution SS NMR spectrum are not consistent with the expected results from the two limit models.

Figure 3a shows the 2D refocused $^{13}C-^{13}C$ INADEQUATE[25] spectrum for the iP3M1B crystal at 233 K. The $T_{1\rho H}$ filter was

Table 1. Closest and Second Closest Contact Distances for C5 Carbons with the Side-chain Carbons of the Neighboring Chains in Unit Cells of (a) the Full Limit Order and (b) the Full Limit Disorder Models

	distance/Å	counter chain and site no.[a]
	(a) Full Limit Order	
C5I	3.83, 3.84	L_d, site 3
C5II	3.52, 3.64	L_d, site 4
	(b) Full Limit Disorder	
C5I	3.83, 3.84	L_d, site 3
	3.72, 4.40	L_u, site 3
C5II	3.52, 3.64	L_d, site 4
	3.56, 3.70	L_u, site 4
C5III	3.94, 4.04	R_u, site 2
	4.06, 4.16	R_d, site 2
C5IV	3.56, 4.02	L_d, site 4
	3.52, 3.84	L_u, site 4

[a] See packing structures in Figure 1.

incorporated into the pulse program, which selectively observes $^{13}C-^{13}C$ bond correlation in the crystalline signals. This low-temperature enhances the NMR signal intensity by a factor of 1.5 compared with that at ambient temperature, and thus, a total experimental time of 9 days achieves adequate INADEQUATE intensities for the iP3M1B crystal even in natural abundance. This technique yields correlation signals between the nuclei connected by a covalent bond. For such spins, the correlation signals appear at summation of chemical shifts of the carbon pairs due to double-quantum (DQ) coherence in the ω_1 dimension, while the signals appear at each single-quantum (SQ) chemical shift in the ω_2 dimension. DQ and SQ shift correlations considerably enhance the spectral resolution. Figure 3a shows all the bond-connected pathways from C1−C2 to C3−C4 and C3−C5 carbons. These pathways are in agreement with the signal assignment in the literature.[15,26,27] Figure 3b shows the expanded side-chain regions of $^{13}C-^{13}C$ correlation peaks between C3 and C4 carbons, and C3 and C5 carbons reflect different packing structures of individual carbons. Among them, C5 signals show eight highly resolved signals. The observation of distinct eight peaks in the 2D shift correlation should be attributed to wide chemical shift dispersions of individual side-chain signals ($\sim$ 2.4 ppm). The obtained number of peaks is consistent with the number of packing structures in the full disorder model for the iP3M1B crystal. On the basis of the chemical shift values acquired by 2D $^{13}C-^{13}C$ INADEQUATE technique, we can obtain populations of the eight peaks by adopting eight Gaussian peaks to the ^{13}C C5 line shapes in the high-resolution SS NMR spectrum. The population is distributed between 8 ± 3 and 21 ± 4% (data are not shown) and is largely different from the 12.5% expected from the full limit-disorder model.[5] The number of resolved peaks and populations of the individual peaks obtained in this study clearly show that local packing structure of the iP3M1B crystal is not full limit order, full limit disorder, or an intermediate between them, but a disordered one. The observed disorders in the packing structures are directly correlated with the polymer chain arrangements in the crystalline lamella.

In summary, we have succeeded in obtaining eight different peaks for the side-chain ^{13}C signals in iP3M1B crystal by applying 2D refocused $^{13}C-^{13}C$ INADEQUATE NMR technique and TPPM decoupling at 233 K. The obtained peak number was well described in terms of different packing structures both of low symmetry of space group and up- and down-orientation disorders in the iP3M1B crystals. This is a preliminary result on the local packing disorders of the polymer crystals by modern SS NMR analysis. We are interested in other,

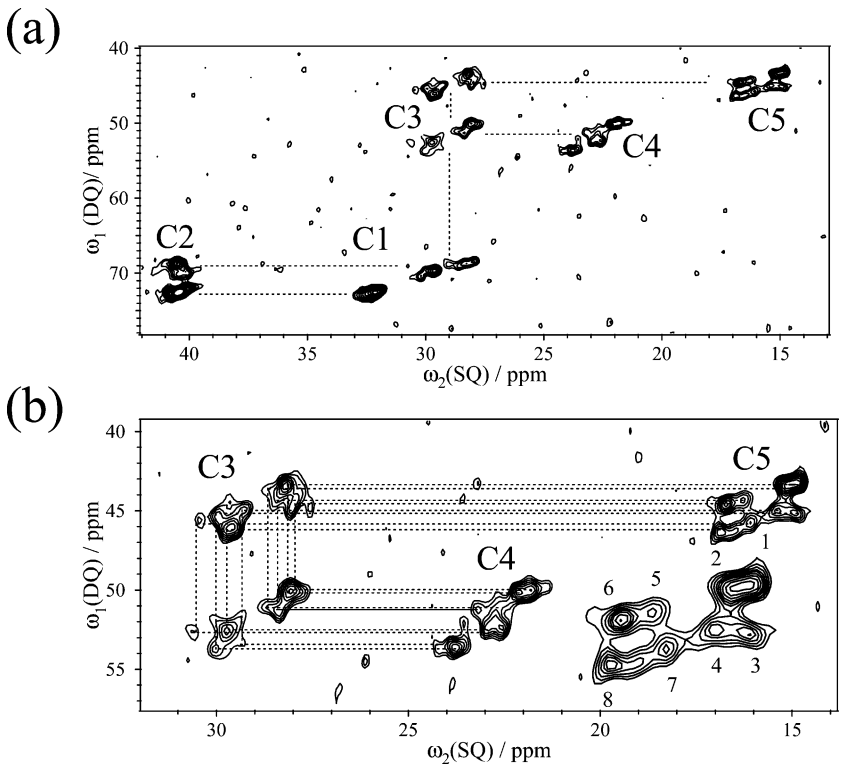

Figure 3. 2D refocused $^{13}C-^{13}C$ INADEQUATE[25] spectrum for whole signals (a) and expanded side-chain signals (b) for the crystallized iP3M1B sample at 233 K. The spectrum was obtained at 75.6 MHz on a BRUKER AVANCE 300 spectrometer, equipped with a 7 mm double-resonance probe. A total of 128 t_1 points with 3072 scans were obtained. The recycle delay was 1.5 s. The τ delay was set to 3.75 ms. The total acquisition time was 9 days. Time averaging was applied using a loop counter in order to suppress changes in NMR conditions. Quadrature detection was achieved by the TPPI method. The other experimental conditions were as follows: MAS frequency, 3 kHz; CP, 1 ms; TPPM decoupling, 70 kHz; 180° pulse, 8.5 μs. The lines represent bond connectivity.

unresolved questions about the iP3M1B crystal structures including the following: (1) Is it possible to assign the multiple peaks to the packing structures? (2) Are individual packing structures mixed in short range or making domain structures in the crystal lamella? (3) If individual packing structures are making domains, what size are the domain structures? (4) How do the polymer chains arrange in the bulk and single-crystal lamella under different crystallization conditions? (5) Is there a relation between local packing structure and molecular dynamics? These questions are common in polymer crystals and have never been unresolved on a molecular level. We are currently performing further experiments on selectively ^{13}C labeled iP3M1B for obtaining inter-site correlations by 2D SS NMR. Some answers related to the above questions will be reported elsewhere.

Acknowledgment. The authors thank for the New Energy and Industrial Technology Development Organization (NEDO) and the Japan Society for the Promotion of Science (JSPS) for support of this work.

References and Notes

(1) Natta, G.; Corradini, P.; Bassi, I. W. *Nuovo Cimento Suppl.* **1960**, *15*, 52−67.
(2) Hikosaka, M.; Seto, T. *Polym. J.* **1973**, *5*, 111−127.
(3) De Rosa, C.; Borriello, A.; Venditto, V.; Corradini, P. *Macromolecules* **1994**, *27*, 3864−3868.
(4) De Rosa, C. *Macromolecules* **2003**, *36*, 6087−6094.
(5) Corradini, P.; Gains, P.; Petraccone, V. *Eur. Polym. J.* **1970**, *6*, 281−291.
(6) Auriemma, F.; Born, R.; Spiess, H. W.; De Rosa, C.; Corradini, P. *Macromolecules* **1995**, *28*, 6902−6910.
(7) VanderHart, D. L.; Alamo, R. G.; Nyden, M. R.; Kim, M. H.; Mandelkern, L. *Macromolecules* **2000**, *33*, 6078−6093.
(8) Natta, G.; Corradini, P.; Bassi, I. W. *Atti Accad, Naz. Lincei, Cl. Sci. Fis. Mat. Nat., Rend.* **1955**, *19*, 404.
(9) Turner-Jones, A.; Aizlewood, J. M. *J. Polym, Sci., Part B* **1963**, *1*, 471−476.
(10) Huguet, M. G. *Macromol. Chem.* **1966**, *94*, 205−227.
(11) Schmidt-Rohr, K.; Spiess, H. W. *Multidimensional Solid-State NMR and Polymers*; Academic Press: London, 1994.
(12) Bunn, A.; Cudby, M. E. A.; Harris, R. K.; Packer, K. J.; Say, B. J. *Polymer* **1982**, *23*, 694−698.
(13) Saito, S.; Moteki, Y.; Nakagawa, M.; Horii, F.; Kitamaru, R. *Macromolecules* **1990**, *23*, 3256−3260.
(14) Caldas, V.; Morin, F. G.; Brown, G. R. *Magn. Reson. Chem.* **1994**, *32*, S72−S79.
(15) Borriello, A.; Busico, V.; De Rosa, C. *Macromolecules* **1995**, *28*, 5679−5680.
(16) De Rosa, C.; Capitani, D.; Cosco, S. *Macromolecules* **1997**, *30*, 8322−8331.
(17) Miyoshi, T.; Hayashi, S.; Kaito, A.; Imashiro, F. *Macromolecules* **2002**, *35*, 2624−2632.
(18) Maring, D.; Whilhelm, M.; Spiess, H. W.; Meurer, B.; Weill, G. *J. Polym. Sci., Part B: Polym. Phys.* **2000**, *38*, 2611−2624.
(19) Andrew, E. R.; Bradbury, A.; Eades, R. *Nature (London)* **1958**, *182*, 1659.
(20) Lowe, I. J. *Phys. Rev. Lett.* **1959**, *2*, 285−287.
(21) Bennett, A. E.; Rienstra, C. M.; Auger, M.; Lakshmi, K. V.; Griffin, R. G. *J. Chem. Phys.* **1995**, *103*, 6951−6958.
(22) Hashi, K.; Shimizu, T.; Goto, A.; Kiyoshi, T.; Matsumoto, S.; Wada, S.; Fujito, T.; Hasegawa, K.; Yoshikawa, M.; Miki, T.; Ito, S.; Hamada, M.; Hayashi, S. *J. Magn. Reson.* **2002**, *156*, 318−321.
(23) Hong, M. *J. Magn. Reson.* **1999**, *136*, 86−91.
(24) Lesage, A.; Auger, C.; Caldarelli, S.; Emsley, L. *J. Am. Chem. Soc.* **1997**, *119*, 7867−7868.
(25) Lesage, A.; Bardet, M.; Emsley, L. *J. Am. Chem. Soc.* **1999**, *121*, 10987−10993.
(26) Hu, W.; Hagihara, H.; Miyoshi, T. *Macromolecules* **2007**, *40*, 1763−1766.
(27) Asakura, T.; Nakayama, N. *Polym. Commun.* **1991**, *32* (7), 213−216.
(28) Tonnelli, A. E. *NMR spectroscopy and Polymer Microstructure*: *the conformational Connection*; VCH Publishers: New York, 1989.
(29) Kirshenbaum, I.; Issacson, R. B.; Druin, M. *Polym. Lett.* **1965**, *3*, 525−528.

MA070518O